



Acetylcholinesterase inhibition, molecular docking and ADME prediction studies of new dihydrofuran-piperazine hybrid compounds

Sait SARI¹ · Mehmet YILMAZ¹

Received: 1 June 2021 / Accepted: 17 August 2021 / Published online: 24 September 2021

© The Author(s), under exclusive licence to Springer Science+Business Media, LLC, part of Springer Nature 2021

Abstract

Novel acrylamide and methacryloyl carrying piperazine-dihydrofuran derivatives (**3a-p**) were designed and obtained from radical cyclizations of unsaturated piperazine derivatives (**1a-f**) with 1,3-dicarbonyl compounds (**2a-c**) mediated by Mn(OAc)₃. Obtained compounds were characterized by spectroscopic methods. In vitro AChE inhibitory activities of **3a-p** were evaluated against AChE (Acetylcholinesterase) by Ellman method and test results showed that **3a**, **3c**, **3j**, and **3l** are the most active AChEI's (AChE inhibitors) of our work with IC₅₀ (half-maximal inhibitory concentration) values of 2.62, 5.29, 1.17, and 3.90 μM, respectively. Furthermore, ligand-protein interactions and inhibitory activity mechanisms of **3a** and **3j** were investigated by molecular docking. Finally, in silico molecular property and ADME predictions (absorption, distribution, metabolism and excretion) of potential AChEI's were predicted by PreADMET and Molinspiration web servers. It can be concluded that the lead compound **3j** show excellent inhibition and satisfactory druglike characteristics.

Keywords Piperazine · Dihydrofuran · Radical cyclization · Acetylcholinesterase inhibition · Molecular docking · ADME

Introduction

Alzheimer's disease (AD) is a neurodegenerative disorder and is one of the main cause of dementia effecting elderly people [1]. The illness is characterized by executive disorders, memory loss, mood disturbances, depression and progressive loss of cognitive abilities [1, 2]. Based on the report of World Health Organization (WHO) about AD, about 36 million people around globe were suffering from dementia until 2010 and this would be increased to 66 million by 2030 [3]. Many theories were suggested to clarify the exact origin of AD such as cholinergic transmission [4], tau protein hyperphosphorylation [5], and beta-amyloid aggregation [6]. Among them, cholinergic

transmission is the most commonly accepted theory and increasing levels of neurotransmitter acetylcholine in the brain is crucial for the treatment of AD [7–9].

Acetylcholinesterase (AChE) is an enzyme in cholinesterase family that catalyzes the rapid hydrolysis of neurotransmitter acetylcholine and terminates impulse transmission at cholinergic synapses [10]. Inhibiting AChE is the most prominent way in the field of AD treatment [11] and there are many commercially available inhibitor drugs such as Donepezil [12], Rivastigmine [13], and Galantamine [14].

Heterocycles bearing nitrogen are important compounds in the field of medicinal chemistry and widely used for their biological properties [15]. Piperazine is considered a privileged structure for its ability of binding to multiple structures with high affinity [16]. Many AChE inhibition studies were performed for piperazine derivatives in literature [17–19].

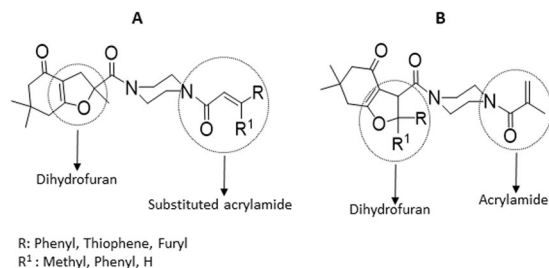
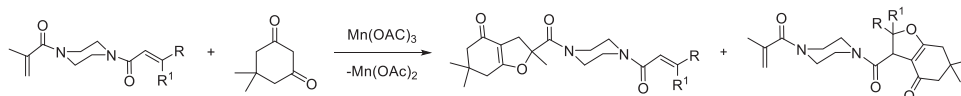
Dihydrofurans are biologically active heterocycles and useful building blocks for naturally occurring compounds such as Sarcophytoside [20] and Clerodin [21]. Dihydrofurans can be obtained by C–C bond forming radical cyclization reactions that occur through the addition of α-carbon radicals to unsaturated systems

Supplementary information The online version contains supplementary material available at <https://doi.org/10.1007/s00044-021-02788-5>.

✉ Mehmet YILMAZ
mehmet.yilmaz@kocaeli.edu.tr

¹ Department of Chemistry, Faculty of Arts and Sciences, Kocaeli University, 41380 Umuttepe, Kocaeli, Turkey

Scheme 1 General reaction scheme of dihydrofuran-piperazine hybrid compounds



Scheme 2 Molecular structures of substituted acrylamide (A) and methacryloyl (B) carrying piperazine-dihydrofuran compounds

[22, 23]. Alpha carbon radicals are generated from active methylene compounds via single electron transferring transition metal salts (Mn^{3+} , Ce^{4+} , Co^{3+} , etc). [24–31]. Our research group has reported the synthesis of dihydrofuran compounds by the radical cyclization of 1,3-dicarbonyl compounds with various unsaturated systems [32–37].

Our research group reported aromatic amide substituted piperazine-dihydrofuran derivatives [38] and good inhibition results were reported (IC_{50} values between 2.24–17.93 μM). Encouraged by the results of our previous work and based on the results that were acquired by many research groups for acrylamides and piperazine compounds over recent years, in present work we studied the radicalic cyclization reaction between aromatic substituted acrylamide and methacryloyl carrying piperazine compounds (**1a–f**) with enolizable 1,3-dicarbonyls (dimedone (**2a**), acetylacetone (**2b**), ethylacetoacetate (**2c**)) via $Mn(OAc)_3$. Radicalic cyclization is possible to occur on both methacryloyl and substituted acrylamide sides depending on steric hindrance and radical stability. Mechanism of this reaction is discussed in Results and Discussion section. General molecular structures of obtained piperazine-dihydrofuran molecules can be seen in Scheme 1 and Scheme 2. Acrylamide and substituted acrylamide carrying piperazine-dihydrofuran products were obtained from these reactions and both of these final products (**3a–p**) were isolated and evaluated for AChE inhibitions.

To further understand the interaction of newly synthesized compounds with AChE, molecular docking studies were performed to investigate the binding modes with AChE (PDB: 4EY7) active site.

Moreover, to predict the druglike potentials of obtained compounds, in silico molecular property and ADME (absorption, distribution, metabolism, excretion) prediction studies were conducted to predict druglikeness of obtained

compounds by using Molinspiration and PreADMET online servers.

Results and discussion

Chemistry

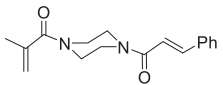
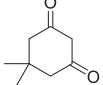
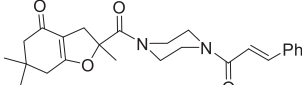
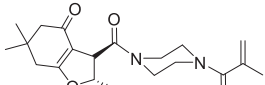
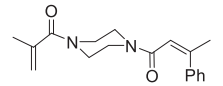
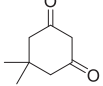
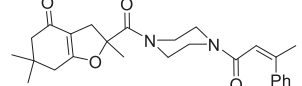
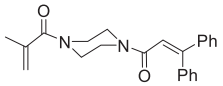
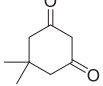
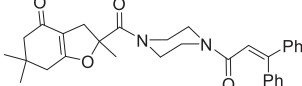
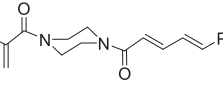
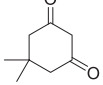
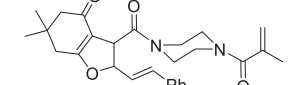
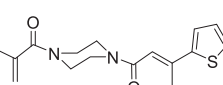
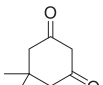
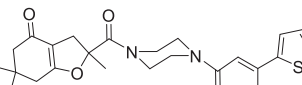
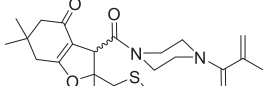
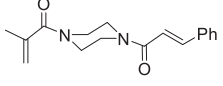
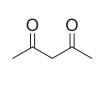
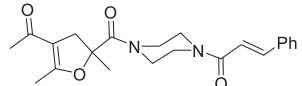
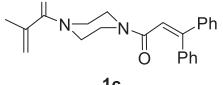
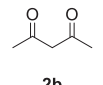
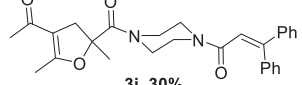
The reactions of acrylamide substituted piperazines (**1a–e**) with dimedone (**2a**) and acetylacetone (**2b**) were given in Table 1. The reaction of piperazine derivative **1a** with dimedone (**2a**) gave piperazine substituted dihydrofuran compounds **3a** (10%) and **3b** (45%) from the cyclization of each acyl group and these compounds were differentiated by their 1H NMR spectra. The 1H NMR spectrum of **3a** shows trans alkene protons at 6.85 and 7.72 ppm as doublet ($J = 15.6$ Hz) for each proton. Also, geminal protons of dihydrofuran ring can be seen at 2.72 and 3.50 ppm as doublet ($J = 15.2$ Hz) for each proton. The terminal alkene protons of **3b** is resonated at 5.03 and 5.20 ppm as two singlet. Also, vicinal protons of dihydrofuran moiety of **3b** can be seen at 4.23 and 6.11 ppm as two doublet ($J = 5.6$ Hz).

Reactions of piperazine derivatives **1b** and **1c** with dimedone (**2a**) gave acrylamide piperazine substituted dihydrofurans **3c** (45%) and **3d** (60%), respectively. Both radical cyclizations occurred through the methacryloyl group, regioselectively. However, the reaction of methacryloyl and (2*E*),(4*E*)-5-phenyl-2,4-pentadienoyl substituted compound **1d** with **2a** formed compound **3e** (20%) through 2,4-pentadienoyl. The exact structure of this compound was clarified with 1H NMR and HMBC spectra. Also, the reaction of **1e** with **2a** gave piperazine substituted dihydrofurans **3f** (10%) and **3g** (40%) from the cyclizations of each acyl group on **1e**. In addition, **3h** (45%) and **3i** (30%) were obtained from the reaction of acetylacetone (**2b**) with **1a** and **1c**, respectively.

As can be seen in Table 2, while piperazine-dihydrofurans **3j** (13%) and **3k** (25%) were obtained from the cyclization (through both acyl groups) of **1a** with **2c**, **3l** (40%) and **3m** (50%) were isolated from the cyclization (only through methacryloyl group) of **1b** and **1c** with **2c**. Similarly, while the reaction of **1f** with **2c** gave piperazine dihydrofurans **3n** (20%) and **3o** (30%), only **3p** (20%) was isolated from the reaction of **1e** with **2c**.

The proposed mechanism for the formation of dihydrofurans is explained in Scheme 3 [39]. According to this mechanism, the enol form of dimedone (A) reacts with $Mn(OAc)_3$ and an alpha carbon radical B is formed, while Mn^{3+} reduces to Mn^{2+} . Alpha carbon radical can interact

Table 1 Synthesis of piperazine-dihydrofurans (3a-i)

Entry	Piperazines	1,3-dicarbonyls	Products and yields ^a
1	 1a	 2a	 3a, 10%  3b, 45%
2	 1b	 2a	 3c, 45%
3	 1c	 2a	 3d, 60%
4	 1d	 2a	 3e, 20%
5	 1e	 2a	 3f, 10%  3g, 40%
6	 1a	 2b	 3h, 45%
7	 1c	 2b	 3i, 30%

a) Isolated yields based on 1,3-dicarbonyl compounds.

with both unsaturated sides of piperazine compound and both of these pathways (*i* and *ii*) are likely to occur at the same time. On pathway *i* an electron from alkene is added to this α -carbon radical and produces the radical carbon intermediate **C**. Intermediate **C** oxidizes to carbocation **D** with $\text{Mn}(\text{OAc})_3$ and intramolecular cyclization of **D** forms the product **E**. On pathway *ii* radicalic cyclization reaction follows similar steps on the other unsaturated site and product **H** is formed.

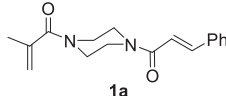
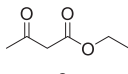
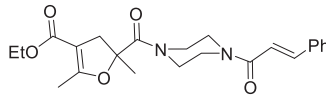
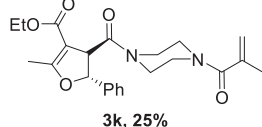
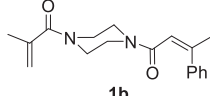
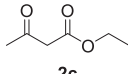
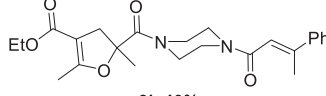
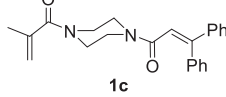
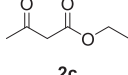
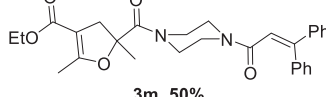
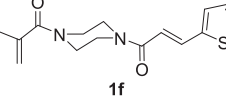
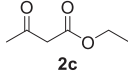
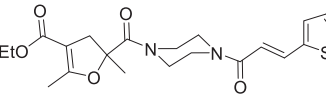
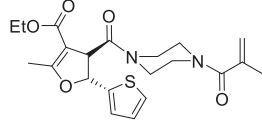
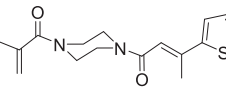
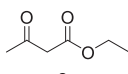
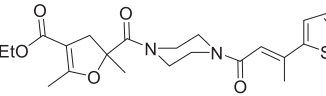
The main reason behind the regioselectivity of **3b** over **3a**, **3g** over **3f**, **3k** over **3j** and **3o** over **3n** is due to stability of radical intermediate **F** over **C** (Scheme 2). Radical intermediate **F** is more stable than **C**, due to aromatic

groups adjacent to carbon radical. Because of this reason, **3b**, **3g**, **3k** and **3o** which formed through pathway *i* were obtained regioselectively and in more yields than their counterparts.

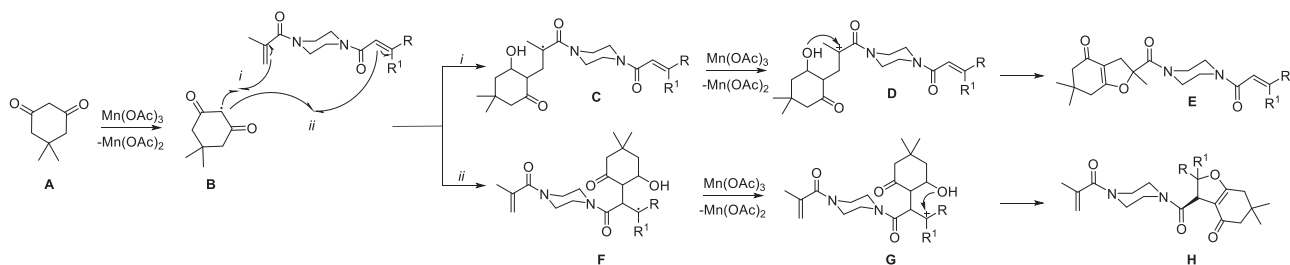
In vitro inhibition results of piperazine-dihydrofuran compounds against AChE

Over recent years there are some works in literature about AChE inhibition of acrylamide and acrylamide containing piperazine compounds. Pan and coworkers described the synthesis of ferulic acid-memoquin hybrids which contain aromatic acrylamide moieties and evaluated their

Table 2 Synthesis of piperazine-dihydrofurans (3j-p)

Entry	Piperazines	1,3-dicarbonyls	Products and yields	
1	 1a	 2c	 3j, 13%	 3k, 25%
2	 1b	 2c	 3l, 40%	
3	 1c	 2c	 3m, 50%	
4	 1f	 2c	 3n, 20%	 3o, 30%
5	 1e	 2c	 3p, 20%	

a) Isolated yields based on 1,3-dicarbonyl compounds.

**Scheme 3** Proposed mechanism of Mn(OAc)₃ mediated radical cyclization

inhibition capabilities against AChE and reported IC₅₀ values between 3.2 and 34.7 μM [40]. Additionally, Shaik and coworkers designed flavone-8-acrylamide compounds and obtained inhibition results between 0.064 and 2.81 μM [41]. Moreover, cinnamic N-benzylpiperidine hybrids were synthesized by Estrada et al. and they obtained good inhibition results (IC₅₀ = 0.26–8.73) [42]. Finally, aromatic acrylamide carrying piperazine derivatives were obtained by Singh and coworkers that show AChE inhibition with IC₅₀ values between 9.91–29.34 μM [43].

In this work, starting unsaturated piperazine derivatives (**1a–f**) used in this study were tested against AChE and they show almost no inhibition (IC₅₀ > 100 μM). On the other hand, in vitro inhibition capabilities of some of the obtained acrylamide carrying piperazine-dihydrofuran compounds were proved to be significantly high. All results compared to standard drugs Donepezil and presented in Table 3.

IC₅₀ values of cinnamoyl acrylamide substituted **3a** and methacryloyl substituted **3b** were calculated and while **3a** has IC₅₀ value of 2.62 μM, **3b** has almost no inhibition (IC₅₀ > 100 μM). Also, IC₅₀ values for compounds **3c** and

Table 3 IC₅₀ values of piperazine-dihydrofuran compounds (3a-p) and Donepezil towards AChE

Compound	IC ₅₀ ± SD (μM) ^a
3a	2.62 ± 0.2
3b	>100
3c	5.29 ± 0.5
3d	11.89 ± 1.3
3e	>100
3f	8.55 ± 0.6
3g	>100
3h	>100
3i	>100
3j	1.17 ± 0.7
3k	>100
3l	3.90 ± 0.5
3m	8.36 ± 0.4
3n	6.11 ± 0.6
3o	>100
3p	8.42 ± 0.3
Donepezil [44]	0.041

^aThe values are mean of three independent experiments ± SD.

3d are 5.19 and 11.89 μM, respectively. By comparing these results it can be seen that inhibition powers in terms of IC₅₀ align as: **3a** > **3c** > **3d**. This is probably due to increasing steric hindrance. By looking at the unsaturated acrylamide moieties of these structures it can be seen that **3a** carries a hydrogen and phenyl group while **3c** bears a methyl and phenyl and **3d** carries two phenyls. These increasing steric hindrances probably make the inhibitor molecule harder to approach to active site of AChE. In addition, while IC₅₀ value of **3f** was calculated as 8.55 μM, it is > 100 μM for methacryloyl containing compound **3g**. Similarly, compound **3e** shows almost no inhibition (IC₅₀ > 100 μM). It is clear that dihydrofuran-piperazine products that bear aromatic acrylamide moieties have much more inhibition power than the products that carry free methacryloyl group. Also, contrary to products obtained from dimedone, **3h** and **3i**, which obtained from the reactions of acetylacetone (**2b**), show no inhibition effects.

Among the piperazine-dihydrofuran compounds obtained from the reactions of ethyl acetoacetate (**2c**) with acrylamide piperazines (**1a-e**), compounds **3j** (IC₅₀ = 1.17 μM) and **3l** (IC₅₀ = 3.90 μM) show the best inhibition effects. Also, IC₅₀ values of **3m**, **3n** and **3p** were calculated as 8.36, 6.11, and 8.42 μM, respectively. By comparing the inhibition powers of **3j**, **3l** and **3m** it can be seen that inhibition capabilities align as **3j** > **3l** > **3m**. Just like the same reason above increasing steric hindrances decreased the inhibition powers of these molecules. On the other hand, similar to compounds mentioned above, methacryloyl containing compounds **3k** and **3o** have almost no inhibition effect (IC₅₀ > 100 μM). In the light of these

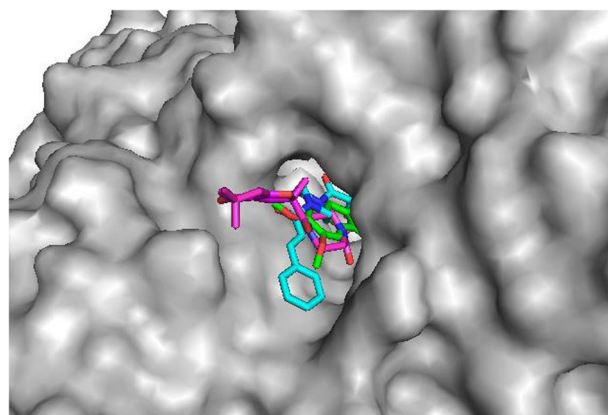


Fig. 1 AChE active site cavity with Donepezil (green), **3a** (magenta) and **3j** (cyan) inside

informations, it is clear that, aromatic moiety carrying acrylamide substituents on piperazine-dihydrofuran compounds have significantly positive effect on inhibitions. Also, it is concluded that, carboxylate substitution on dihydrofuran group increases inhibition efficiency than other substitutions on dihydrofurans. Based on these results, compound **3j** is selected as our lead compound.

Molecular docking results of selected piperazine-dihydrofuran compounds (**3a** and **3j**)

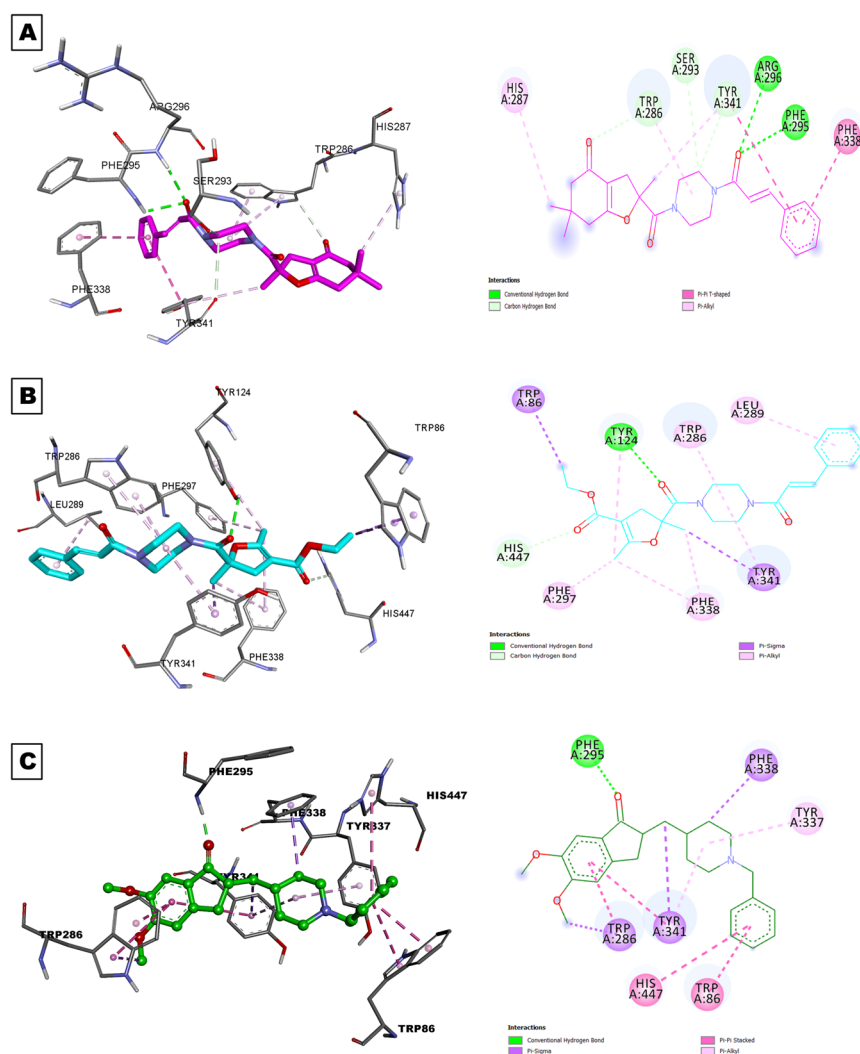
AChE active site is 20 Å deep gorge that is located at the bottom of the enzyme molecule. This active site consists of several subsites. These sites and important residues they contain are; catalytic triad (SER203, HIS447, GLU334), anionic subsite (TRP86, TYR133, GLU202, GLY448, ILE451), oxyanion hole (GLY121, GLY122, ALA204), acyl binding pocket (TRP236, PHE295, PHE297, PHE338) and peripheral anionic subsite (ASP74, TYR124, SER125, TRP286, TYR337, TYR341) [45].

Molecular docking studies were performed on two of our most potent inhibitor compounds (**3a** and **3j**) and Donepezil. Docking procedure was validated by re-docking the native ligand Donepezil to target AChE. Near perfect alignment with a RMSD value of 0.340 was obtained from validation results. Binding score of native ligand Donepezil is −12.2 Kcal/mol. Binding energies for top docking poses of ligands **3a** and **3j** are −9.6 and −10.4 Kcal/mol, respectively. Superpositioned docking poses of **3a**, **3j**, and Donepezil in AChE active site cavity can be seen in Fig. 1 and shows good alignment with native ligand Donepezil (Fig. 1).

Ligand-protein interactions of top binding poses of ligands **3a**, **3j** and Donepezil were given in Fig. 2.

By investigating the ligand-protein interactions of Donepezil, it can be seen that N-benzyl moiety of Donepezil made π-π interactions with aromatic groups of HIS447 and TRP86. Also, piperidine ring of Donepezil interacts with

Fig. 2 Ligand-protein interactions of **3a** (A), **3j** (B) and Donepezil (C)



aromatic moieties of TYR341, TYR337, and PHE338 through π -alkyl and π - σ interactions. In addition, carbonyl oxygen forms a hydrogen bonding with PHE295. Benzene and methoxy groups of Donepezil interact with TRP286 through π - π and π - σ interactions, respectively. Similarly TYR341 residue interacts with benzene and $-CH_2$ bridge through π - π and π - σ interactions, respectively.

By investigating the docking mod of **3a** similar residue interactions with Donepezil can be seen. One of the methyl groups of dimedone ring of **3a** forms π -alkyl interactions with aromatic moiety of HIS287. Also, dimedone carbonyl forms a carbon-hydrogen bond with TRP286. Methyl group on dihydrofuran ring interacts with TYR341 through a hydrophobic π -alkyl interaction. Piperazine ring forms hydrophobic π -alkyl interactions with aromatic moieties of TRP286 and carbon-hydrogen bonds with SER293 and TYR341. In addition, acrylamide carbonyl forms hydrogen bondings with PHE295 and ARG296. Finally, aromatic moiety of acrylamide group forms π - π interactions with TYR341 and PHE338.

Also, the lead compound **3j**, interacts with similar residues like reference drug Donepezil. It can be seen that ethyl carboxylate moiety forms π - σ interaction with aromatic moiety of TRP86. Also, ester carbonyl forms a Carbon-Hydrogen bond with HIS447. Methyl groups on dihydrofuran ring made π -alkyl interactions with PHE338, TYR124, and PHE297, also one methyl group on dihydrofuran ring interacts with TYR341 through a π - σ interaction. Moreover, carbonyl next to dihydrofuran ring forms a hydrogen bond with TYR124. Additionally, piperazine ring interacts with TYR341 and TRP286 through π -alkyl interactions. Finally, the aromatic ring of cinnamoyl group interacts with LEU289 through a π -alkyl interaction.

By considering the ligand-protein interactions of top binding modes of ligands it can be seen that docking results show similar residue interactions like reference drug Donepezil and support in vitro inhibition results.

Table 4 In silico molecular property predictions for AChEI's

Code	MW ^a	MiLogP ^b	HBA ^c	HBD ^d	Nviol ^e	TPSA ^f	MVol ^g
Rule	<500	≤5	≤10	≤5	≤1	<160 Å ²	
3a	422.52	3.26	6	0	0	66.92	398.16
3c	436.55	3.14	6	0	0	66.92	414.72
3d	498.62	4.36	6	0	0	66.92	469.57
3f	442.58	3.04	6	0	0	66.92	405.43
3j	412.49	3.15	7	0	0	76.16	384.68
3l	426.51	3.03	7	0	0	76.16	401.24
3m	488.58	4.25	7	0	0	76.16	456.09
3n	418.51	2.87	7	0	0	76.16	375.39
3p	432.54	2.93	7	0	0	76.16	391.95
Donepezil	379.50	4.10	4	0	0	38.78	367.89

a: Molecular weight (MW); b: logarithm of octanol-water partition coefficient (MiLogP); c: Number of hydrogen bond acceptors (HBA); d: Number of hydrogen bond donors (HBD); e: Lipinski rule violations (nviol); f: Topological polar surface area (TPSA); g: Molecular volume (MVol).

Table 5 In silico ADME predictions of AChEI's

Code	Absorption			Distribution	
	Human intestinal absorption (%)	In vitro Caco-2 cell permeability (nm/s)	In vitro MDCK cell permeability (nm/s)	In vitro skin permeability (log Kp, cm/h)	In vitro plasma protein binding PPB (%)
Rule	0–20 (poor) 20–70 (moderate) 70–100 (well)	<4 (low), 4–70 (moderate), >70 (high)	<25 (low) 25–500 (moderate) >500 (high)		>90 (strongly bound) <90 (weakly bound)
3a	98.00	49.67	0.06	−3.29	82.79
3c	97.86	50.32	0.06	−3.25	84.87
3d	97.48	52.53	0.04	−2.39	90.62
3f	99.52	53.17	0.07	−3.85	84.09
3j	98.95	45.52	0.11	−3.17	76.39
3l	98.87	46.87	0.08	−3.14	79.85
3m	97.69	50.02	0.04	−2.36	89.16
3n	98.65	50.25	0.17	−3.75	72.94
3p	98.96	51.48	0.11	−3.71	78.50
Donepezil	97.95	55.52	0.14	−3.04	84.61

In silico molecular property and ADME prediction results

ADME properties are one of the main reasons for a drug candidate to fail in clinical trials. In silico molecular property and ADME predictions of obtained piperazine-dihydrofuran compounds which have inhibition powers against AChE (AChEI's) (**3a**, **3c**, **3d**, **3f**, **3j**, **3l**, **3m**, **3n**, and **3p**) and reference drug Donepezil were carried out using Molinspiration (<https://www.molinspiration.com/>) and Pre-ADMET (<https://preadmet.bmdrc.kr/>) webserver in order to predict druglikeness of these molecules. According to Lipinski's rule [46] a drug candidate can possess no more than one violation of the following criteria: (i) Hydrogen bond acceptors must be ≤10. (ii) Hydrogen bond donors must be ≤5 (iii) Molecular weight (MW) must be less than

500 D and (iv) Octanol-water partition coefficient (MilogP) of the molecule must be ≤5.

As can be seen in Table 4 Piperazine-dihydrofuran compounds show no violation against Lipinski's rule.

Moreover, in silico ADME prediction results of AChEI's were given in Table 5 [47].

Human intestinal absorption (HIA) indicates gastrointestinal permeation across membranes for drugs which taken orally. All AChEI compounds show great HIA values over 97%.

In vitro Caco-2 cell permeability is an indication of intestinal absorption of drugs. According to our results all AChEI's show moderate permeations between 41–53 nm/s.

In vitro MDCK cell permeability test utilizes canine kidney cells to test permeability. All AChEI test compounds show low permeation values.

Skin permeability is a factor that indicates delivery of a drug through transdermal administration. All AChEI's compounds show negative permeability which shows transdermal administration is not suitable for these molecules.

In vitro plasma protein binding (PPB) indicates percentage of a drug is bound to blood plasma proteins. Our AChEI's show binding values less than 90% except **3d**. This means they can efficiently diffuse to cell membranes.

Conclusion

In the presented work, new piperazine-dihydrofuran compounds (**3a-p**) were designed and synthesized from $\text{Mn}(\text{OAc})_3$ mediated radical cyclizations of 1,3-dicarbonyl compounds (**2a-c**) and acrylamide carrying piperazine derivatives (**1a-f**) in low and medium yields. AChE inhibition capabilities of starting piperazine derivatives (**1a-f**) and piperazine-dihydrofuran compounds (**3a-p**) were tested. Although many of the piperazine-dihydrofuran compounds (**3a**, **3c**, **3d**, **3f**, **3j**, **3l**, **3m**, **3n**, and **3p**) show inhibition capabilities against AChE, starting acylated piperazine compounds (**1a-f**) show no inhibition effects. While piperazine-dihydrofuran compounds containing aromatically substituted acrylamide moieties have high inhibition effects against AChE (IC_{50} values ranging from 1.17 to 11.89 μM), methacryloyl carrying piperazine-dihydrofuran compounds (**3b**, **3g**, **3h**, **3i**, **3k**, and **3o**) show almost no inhibitions. Also, carboxy substituted piperazine-dihydrofuran compounds show higher inhibition effects than other piperazine-dihydrofurans, especially **3j** ($\text{IC}_{50} = 1.17 \mu\text{M}$) which is our lead compound. In addition, molecular docking studies were performed with the lead compound **3j** and the other most potent AChEI **3a** to investigate ligand-protein interactions and binding energies. Calculated docking results were compared to standard drug Donepezil. Binding scores of Donepezil is -12.2 Kcal/mol and -9.6 , -10.4 Kcal/mol for **3a** and **3j** respectively. Finally, in silico molecular property analysis and ADME prediction studies show that our lead compound **3j** and other AChEI's have satisfactory druglike characteristics. Summarily, the lead piperazine-dihydrofuran compound **3j** which carries phenyl substituted acrylamide moiety and carboxylate group have excellent AChE inhibition and satisfactory druglike characteristics. This compound has the potential to be a drug candidate and can be further modified to increase the activity against Acetylcholinesterase.

Experimental

All reagents and solvents are commercially available and analytically pure unless otherwise stated. AChE (from electric eel, type V-S), acetylthiocholine iodide (ATCI), 5,5'-dithiobis(2-nitrobenzoic acid) (DTNB) were supplied

from Sigma Aldrich. Radical oxidant $\text{Mn}(\text{OAc})_3$ was synthesized by electrochemical method [34].

^1H NMR and ^{13}C NMR spectra were recorded on a Varian Mercury-400 High performance Digital FT-NMR and Varian Oxford NMR300 spectrometers. HRMS spectra were obtained on an Agilent 1200/6210 LC/MS spectrophotometer. IR spectra (ATR) were obtained with a Bruker Tensor27 spectrophotometer in the $400\text{--}4000 \text{ cm}^{-1}$ range with 2 cm^{-1} resolutions. UV absorbances were recorded by Rigol Ultra-3000 UV-Vis Spectrophotometer. Melting points were determined on a Gallenkamp capillary melting point apparatus. Thin-layer chromatography (TLC) was performed on Merck aluminum-packed silica gel plates. Purification of products was performed by column chromatography on silica gel (Merck silica gel 60, 40–60 μm) or preparative TLC on silica gel of Merck (PF254-366 nm).

General synthesis procedure and spectroscopic data of piperazine dihydrofuran compounds (**3a-p**)

Starting unsaturated piperazine derivatives (**1a-f**) were obtained according to our previously reported work [48]. All piperazine-dihydrofuran compounds (**3a-p**) were synthesized by the general method described below.

$[\text{Mn}(\text{OAc})_3] \cdot 2\text{H}_2\text{O}$ (2 mmol, 0.53 g) in 15 mL glacial acetic was heated to $80 \text{ }^\circ\text{C}$ until dissolved. After that, the solution temperature was cooled to $65 \text{ }^\circ\text{C}$ and a solution of 1,3-dicarbonyl compound (**2a-c**) (1 mmol) and piperazine compound (**1a-f**) (1.2 mmol) in 3 mL of acetic acid was added. The mixture was stirred and the disappearance of the initial dark brown indicated that the reaction was finished (10-30 min). After that, water was added and the reaction mixture was extracted with CHCl_3 ($3 \times 20 \text{ mL}$). The combined organic phase was neutralized with saturated NaHCO_3 solution, dried over anhydrous Na_2SO_4 , and evaporated. The crude product was purified with column chromatography or preparative TLC (chloroform:acetone (85:15) as eluent).

2-(4-cinnamoylpiperazine-1-carbonyl)-2,6,6-trimethyl-3,5,6,7-tetrahydrobenzofuran-4(2H)-one (**3a**)

It was obtained as a yellow oil; yield: 10% (42 mg); IR (ATR) ν_{max} 3071, 2961, 2921, 2850, 1725 (C=O), 1652 (C=O), 1630 (C=C), 1226, 1192, 752, 692 (aromatic C-H) cm^{-1} ; ^1H NMR (400 MHz, CDCl_3) δ (ppm): 7.72 (1H, d, $J = 15.6 \text{ Hz}$, H_{olef}), 7.53 (2H, dd, $J = 5, 2, 2 \text{ Hz}$, arom. CH), 7.37 (3H, dd, $J = 5.2, 2 \text{ Hz}$, arom. CH), 6.85 (1H, d, $J = 15.6 \text{ Hz}$, H_{olef}), 3.87-3.58 (8H, broad), 3.50 (1H, d, $J = 15.2 \text{ Hz}$, Ha-3), 2.72 (1H, d, $J = 15.2 \text{ Hz}$, Hb-3), 2.30 (2H, d, $J = 16.0 \text{ Hz}$), 2.27 (2H, s), 1.63 (3H, s, $-\text{CH}_3$), 1.13 (3H, s, $-\text{CH}_3$), 1.11 (3H, s, $-\text{CH}_3$); ^{13}C NMR (100 MHz, CDCl_3) δ (ppm): 194.6

(C=O), 173.0 (C=C, C-7a), 169.8 (C=O), 165.7 (C=O), 143.7 (C=C), 134.9, 129.9, 128.9, 127.8, 116.3 (C=C), 111.4 (C=C, C-3a), 91.9, 50.9, 46.0, 37.8, 37.6, 34.3, 28.7 (–CH₃), 28.6 (–CH₃), 26.2 (–CH₃); HRMS (ESI) (m/z) Calcd for C₂₅H₃₀N₂O₄ 423.22783 found: 423.22835 (M + H)⁺

Trans-3-(4-methacryloylpiperazine-1-carbonyl)-6,6-dimethyl-2-phenyl-3,5,6,7-tetrahydrobenzofuran-4(2H)-one (3b)

It was obtained as a yellow oil; yield: 45% (190 mg); IR (ATR) ν_{\max} 3054, 2961, 2952, 2868, 1719 (C=O), 1637 (C=O), 1610 (C=C), 1228, 1208, 760, 706 (arom. CH) cm⁻¹; ¹H NMR (400 MHz, CDCl₃) δ (ppm): 7.41–7.33 (3H, m, arom. CH), 7.25–7.23 (2H, m, arom. CH), 6.11 (1H, d, *J* = 5.6 Hz, H-2), 5.20 (1H, s, H_{olef.}), 5.03 (1H, s, H_{olef.}), 4.23 (1H, d, *J* = 5.6 Hz, H-3), 4.01–3.30 (8H, broad), 2.47 (2H, d, *J* = 16.0 Hz), 2.26 (2H, d, *J* = 16.0 Hz), 1.94 (3H, s, –CH₃), 1.15 (3H, s, –CH₃), 1.04 (3H, s, –CH₃); ¹³C NMR (100 MHz, CDCl₃) δ (ppm): 193.9 (C=O), 178.1 (C=C, C-7a), 171.3 (C=O), 170.3 (C=O), 140.0 (C=C), 139.7, 129.1, 128.9, 125.52, 116.0 (C=C), 112.1 (C=C, C-3a), 90.5, 51.1, 49.9, 47.2, 44.2, 37.9, 34.4, 28.9 (–CH₃), 28.3 (–CH₃), 20.4 (–CH₃); HRMS (ESI) (m/z) Calcd for C₂₅H₃₀N₂O₄ 423.22783 found: 423.22835 (M + H)⁺

2,6,6-trimethyl-2-(4-(3-phenylbut-2-enoyl)piperazine-1-carbonyl)-3,5,6,7-tetrahydrobenzofuran-4(2H)-one (3c)

It was obtained as a yellow oil; yield: 45% (196 mg); IR (ATR) ν_{\max} 3058, 2961, 2921, 2850, 1725 (C=O), 1652 (C=O), 1630 (C=C), 1225, 1192, 752, 692 (arom. CH) cm⁻¹; ¹H NMR (400 MHz, CDCl₃) δ (ppm): 7.45 (2H, dd, *J* = 8.4, 2 Hz, arom. CH), 7.39–7.33 (3H, m, arom. CH), 6.26 (1H, s, H_{olef.}), 3.80–3.54 (8H, broad), 3.49 (1H, d, *J* = 15.2 Hz, Ha-3), 2.71 (1H, d, *J* = 15.2 Hz, Hb-3), 2.29 (4H, s), 2.24 (3H, s, –CH₃), 1.62 (3H, s, –CH₃), 1.12 (3H, s, –CH₃), 1.10 (3H, s, –CH₃); ¹³C NMR (100 MHz, CDCl₃) δ (ppm): 194.6 (C=O), 173.0 (C=C, C-7a), 169.75 (C=O), 167.31 (C=O), 141.4 (C=C), 128.6, 128.5, 126.0, 118.8, 116.1 (C=C), 111.4 (C=C, C-3a), 91.9, 50.9, 46.0, 43.7, 37.8, 34.3, 28.7 (–CH₃), 28.6 (–CH₃), 26.3 (–CH₃), 18.06 (–CH₃); HRMS (ESI) (m/z) Calcd for C₂₆H₃₂N₂O₄ 437.24348 found 437.24483 (M + H)⁺

2-(4-(3,3-diphenylacryloyl)piperazine-1-carbonyl)-2,6,6-trimethyl-3,5,6,7-tetrahydrobenzofuran-4(2H)-one (3d)

It was obtained as a yellow oil; yield: 60% (300 mg); IR (ATR) ν_{\max} 3058, 2961, 2925, 2872, 1714 (C=O), 1632 (C=O), 1604 (C=C), 1201, 1006, 752, 701 (arom. CH) cm⁻¹; ¹H NMR (400 MHz, CDCl₃) δ (ppm): 7.37–7.26 (10H,

m, arom. CH), 6.30 (1H, s, H_{olef.}), 3.64–2.98 (8H, broad), 3.37 (1H, d, *J* = 15.2 Hz, Ha-3), 2.65 (1H, d, *J* = 15.2 Hz, Hb-3), 2.25 (2H, d, *J* = 16.4 Hz), 2.20 (2H, d, *J* = 16.4 Hz), 1.53 (3H, s, –CH₃), 1.11 (3H, s, –CH₃), 1.08 (3H, s, –CH₃); ¹³C NMR (100 MHz, CDCl₃) δ (ppm): 194.5 (C=O), 173.0 (C=C, C-7a) 169.4 (C=O), 167.34 (C=O), 147.9 (C=C), 140.5, 138.7, 129.5, 128.8, 128.4, 128.4, 128.0, 111.4 (C=C), 110.0 (C=C, C-3a), 91.7, 50.88, 46.1, 45.5, 42.9, 41.1, 37.7, 37.5, 34.2, 28.72 (–CH₃), 28.6 (–CH₃), 26.16 (–CH₃); HRMS (ESI) (m/z) Calcd for C₃₁H₃₄N₂O₄ 499.25913 found 499.26110 (M + H)⁺

Trans-3-(4-methacryloylpiperazine-1-carbonyl)-6,6-dimethyl-2-styryl-3,5,6,7-tetrahydrobenzofuran-4(2H)-one (3e)

It was obtained as a yellow oil; yield: 20% (89 mg); IR (ATR) ν_{\max} 3067, 2965, 2925, 2854, 1734 (C=O), 1646 (C=O), 1626 (C=C), 1191, 1090, 754, 695 (arom. CH) cm⁻¹; ¹H NMR (400 MHz, CDCl₃) δ (ppm): 7.31 (5H, m, arom. CH), 6.66 (1H, d, *J* = 15.6 Hz, H_{olef.}), 6.20 (1H, dd, *J* = 15.6, 7.6 Hz, H_{olef.}), 5.74 (1H, t, *J* = 6.4, H-2), 5.21 (1H, s, H_{olef.}), 5.04 (1H, s, H_{olef.}), 3.71 (1H, d, *J* = 6.4 Hz, H-3), 3.98–3.26 (8H, broad), 2.41 (2H, d, *J* = 17.0 Hz) 2.20 (2H, d, *J* = 16.4 Hz), 1.96 (3H, s, –CH₃), 1.14 (3H, s, –CH₃) 1.12 (3H, s, –CH₃); ¹³C-NMR (100 MHz, CDCl₃), δ (ppm): 193.9 (C=O), 177.7 (C=C, C-7a), 171.3 (C=O), 170.2 (C=O), 140.0 (C=C), 135.3, 134.1, 128.8 (C=C), 128.7, 128.6, 126.8, 125.4 (C=C), 115.9 (C=C), 112.1 (C=C, C-3a), 90.23, 51.06, 47.6, 46.4, 42.3, 37.9, 34.3, 28.7 (–CH₃), 28.4 (–CH₃), 20.4 (–CH₃); HRMS (ESI) (m/z) Calcd for C₂₇H₃₂N₂O₄ 449.24348 found 449.24527 (M + H)⁺

2,6,6-trimethyl-2-(4-(3-(thiophen-2-yl)but-2-enoyl)piperazine-1-carbonyl)-3,5,6,7-tetrahydrobenzofuran-4(2H)-one (3f)

It was obtained as a yellow oil; yield: 10% (44 mg); IR (ATR) ν_{\max} 3071, 2965, 2921, 2863, 1716 (C=O), 1650 (C=O), 1621 (C=C), 1194, 1017, 759, 692 (arom. CH) cm⁻¹; ¹H NMR (400 MHz, CDCl₃) δ (ppm): 7.28 (1H, d, *J* = 0.8 Hz, arom. CH), 7.21 (1H, dd, *J* = 4.0, 0.8 Hz, arom. CH), 7.03 (1H, dd, *J* = 5.2, 4.0 Hz, arom. CH), 6.38 (1H, s, H_{olef.}), 3.79–3.55 (8H, broad), 3.50 (1H, d, *J* = 15.2 Hz, Ha-3), 2.72 (1H, d, *J* = 15.2 Hz, Hb-3), 2.34 (3H, s, –CH₃), 2.31 (2H, d, *J* = 16.0 Hz), 2.25 (2H, s), 1.62 (3H, s, –CH₃), 1.12 (3H, s, –CH₃), 1.11 (3H, s, –CH₃); ¹³C-NMR (100 MHz, CDCl₃), δ (ppm): 194.6 (C=O), 172.9 (C=C, C-7a), 171.9 (C=O), 169.7 (C=O), 145.1 (C=C), 127.8, 125.8, 125.6, 116.1 (C=C), 111.5 (C=C, C-3a), 91.9, 50.9, 46.3, 45.8, 37.8, 37.5, 34.2, 29.6 (–CH₃), 28.6 (–CH₃), 26.2 (–CH₃), 17.8 (–CH₃); HRMS (ESI) (m/z) Calcd for C₂₄H₃₀N₂O₄S 443.19990 found 443.20162 (M + H)⁺

3-(4-methacryloylpiperazine-1-carbonyl)-2,6,6-trimethyl-2-(thiophen-2-yl)-3,5,6,7-tetrahydrobenzofuran-4(2H)-one (3g)

It was obtained as a yellow oil; yield: 40% (177 mg); IR (ATR) ν_{\max} 3071, 2956, 2921, 2859, 1736 (C=O), 1643 (C=O), 1610 (C=C), 1194, 1024, 755, 700 (arom CH) cm^{-1} ; ^1H NMR (400 MHz, CDCl_3) δ (ppm): 7.28 (1H, d, $J = 4.4$ Hz, arom. CH), 7.00–6.97 (2H, m, arom. CH), 5.22 (1H, s, H_{olef}), 5.05 (1H, s, H_{olef}), 4.44 (1H, s, H-2), 3.60–3.52 (8H, m), 2.40 (2H, d, $J = 16.4$ Hz), 2.27 (2H, d, $J = 16.4$ Hz), 1.95 (3H, s, $-\text{CH}_3$), 1.83 (3H, s, $-\text{CH}_3$), 1.46 (3H, s, $-\text{CH}_3$), 1.21 (3H, s, $-\text{CH}_3$); ^{13}C -NMR (100 MHz, CDCl_3) δ (ppm): 194.1 (C=O), 175.6 (C=C, C-7a), 171.3 (C=O), 167.94 (C=O), 148.9, 139.9 (C=C), 127.0, 125.4, 123.2, 116.1 (C=C), 112.7 (C=C, C-3a), 90.8, 53.0, 50.73, 46.28, 42.66, 37.7, 34.6, 28.7 ($-\text{CH}_3$), 28.4 ($-\text{CH}_3$), 23.8 ($-\text{CH}_3$), 20.45 ($-\text{CH}_3$); HRMS (ESI) (m/z) Calcd for $\text{C}_{24}\text{H}_{30}\text{N}_2\text{O}_4\text{S}$ 443.19990 found 443.20162 (M + H)⁺

1-(4-(4-acetyl-2,5-dimethyl-2,3-dihydrofuran-2-carbonyl)piperazin-1-yl)-3-phenylprop-2-en-1-one (3h)

It was obtained as a yellow oil; yield: 45% (172 mg); IR (ATR) ν_{\max} 3076, 2965, 2912, 2845, 1714 (C=O), 1632 (C=O), 1602 (C=C), 1230, 1022, 756, 708 (arom. CH) cm^{-1} ; ^1H NMR (400 MHz, CDCl_3) δ (ppm): 7.72 (1H, d, $J = 15.2$ Hz, H_{olef}), 7.54–7.52 (2H, m, arom. CH), 7.41–7.36 (3H, m, arom. CH), 7.86 (1H, d, $J = 15.2$ Hz, H_{olef}), 3.78 (1H, d, $J = 14.8$ Hz, Ha-3), 3.98–3.56 (8H, broad), 2.79 (1H, d, $J = 14.8$ Hz, Hb-3), 2.23 (3H, s, $-\text{CH}_3$), 2.20 (3H, s, $-\text{CH}_3$), 1.62 (3H, s, $-\text{CH}_3$); ^{13}C -NMR (100 MHz, CDCl_3) δ (ppm): 191.0 (C=O), 177.5 (C=C, C-5), 169.7 (C=O), 165.5 (C=O), 143.7 (C=C), 134.9, 129.9, 128.8, 127.8, 116.3 (C=C), 114.2 (C=C, C-4), 88.6, 46.5, 44.3, 42.0, 29.6 ($-\text{CH}_3$), 26.1 ($-\text{CH}_3$), 24.5 ($-\text{CH}_3$), 14.84 ($-\text{CH}_3$); HRMS (ESI) (m/z) Calcd for $\text{C}_{22}\text{H}_{26}\text{N}_2\text{O}_4$ 383.19653 found 383.19745 (M + H)⁺

1-(4-(4-acetyl-2,5-dimethyl-2,3-dihydrofuran-2-carbonyl)piperazin-1-yl)-3,3-diphenylprop-2-en-1-one (3i)

It was obtained as a yellow oil; yield: 30% (137 mg); IR (ATR) ν_{\max} 3058, 2978, 2925, 2863, 1725 (C=O), 1630 (C=O), 1604 (C=C), 1239, 1026, 759, 701 (arom. CH) cm^{-1} ; ^1H NMR (400 MHz, CDCl_3) δ (ppm): 7.33 (10H, m, arom. CH), 6.30 (1H, s, H_{olef}), 3.69 (1H, d, $J = 15.2$ Hz, Ha-3), 3.74–2.77 (8H, broad), 2.71 (1H, d, $J = 15.2$ Hz, Hb-3), 2.17 (6H, s, $-\text{CH}_3$), 1.63 (3H, s, $-\text{CH}_3$); ^{13}C -NMR (100 MHz, CDCl_3) δ (ppm): 192.0 (C=O),

176.5 (C=C, C-5), 171.7 (C=O), 167.5 (C=O), 140.5, 138.7, 129.5, 128.8, 128.8, 128.4, 128.4, 128.1, 120.1, 117.5 (C=C), 114.8 (C=C, C-4), 88.5, 45.8, 41.9, 27.0, 25.3 ($-\text{CH}_3$), 23.4 ($-\text{CH}_3$), 12.2 ($-\text{CH}_3$); HRMS (ESI) (m/z) Calcd for $\text{C}_{28}\text{H}_{30}\text{N}_2\text{O}_4$ 459.22783 found 459.22902 (M + H)⁺

Ethyl 5-(4-cinnamoylpiperazine-1-carbonyl)-2,5-dimethyl-4,5-dihydrofuran-3-carboxylate (3j)

It was obtained as a yellow oil; yield: 13% (51 mg); IR (ATR) ν_{\max} 3067, 2969, 2930, 2872, 1736 (C=O), 1643 (C=O), 1608 (C=C), 1194, 1090, 761, 701 (arom. CH) cm^{-1} ; ^1H NMR (400 MHz, CDCl_3) δ (ppm): 7.71 (1H, d, $J = 15.2$ Hz, H_{olef}), 7.53 (2H, dd, $J = 5.2$, 2 Hz arom. CH), 7.36 (3H, dd, $J = 5.2$, 2 Hz arom. CH), 6.87 (1H, d, $J = 15.2$ Hz, H_{olef}), 4.15 (2H, q, $J = 7.2$ Hz, $-\text{OCH}_2\text{CH}_3$), 3.92–3.55 (8H, broad), 3.61 (1H, d, $J = 15.2$ Hz, Ha-3), 2.74 (1H, d, $J = 15.2$ Hz, Hb-3), 2.21 (3H, s, $-\text{CH}_3$), 1.59 (3H, s, $-\text{CH}_3$), 1.27 (3H, t, $J = 7.2$ Hz, $-\text{OCH}_2\text{CH}_3$); ^{13}C -NMR (100 MHz, CDCl_3) δ (ppm): 170.5 (C=C, C-2), 165.7 (C=O), 165.5 (C=O), 164.5 (C=O), 143.5 (C=C), 134.9, 129.8, 129.0, 128.8, 127.8, 125.4, 116.4 (C=C), 102.4 (C=C, C-3), 88.3, 59.7, 46.2, 43.5, 42.2, 41.2, 26.0 ($-\text{CH}_3$), 14.3 ($-\text{CH}_3$), 14.1 ($-\text{CH}_3$); HRMS (ESI) (m/z) Calcd for $\text{C}_{23}\text{H}_{28}\text{N}_2\text{O}_5$ 413.20710 found 413.20625 (M + H)⁺

Trans-Ethyl 4-(4-methacryloylpiperazine-1-carbonyl)-2-methyl-5-phenyl-4,5-dihydrofuran-3-carboxylate (3k)

It was obtained as a yellow oil; yield: 25% (105 mg); IR (ATR) ν_{\max} 3026, 2966, 2930, 2870, 1740 (C=O), 1638 (C=O), 1610 (C=C), 1200, 1025, 750, 700 (arom. CH) cm^{-1} ; ^1H NMR (400 MHz, CDCl_3) δ (ppm): 7.42–7.33 (3H, m, arom. CH), 7.29–7.26 (2H, m, arom. CH), 5.67 (1H, d, $J = 7.2$ Hz, H-5), 5.21 (1H, s, H_{olef}), 5.02 (1H, s, H_{olef}), 4.35 (1H, d, $J = 7.2$ Hz, H-4), 4.15 (2H, q, $J = 7.2$ Hz, $-\text{OCH}_2\text{CH}_3$), 3.80–3.30 (8H, broad), 2.35 (3H, s, $-\text{CH}_3$), 1.94 (3H, s, $-\text{CH}_3$), 1.26 (3H, t, $J = 7.2$ Hz, $-\text{OCH}_2\text{CH}_3$); ^{13}C -NMR (100 MHz, CDCl_3) δ (ppm): 171.7 (C=C, C-2), 171.2 (C=O), 169.5 (C=O), 165.0 (C=O), 139.9 (C=C), 139.7, 129.0, 128.8, 127.8, 125.4, 116.0 (C=C), 103.65 (C=C, C-3), 87.3, 59.9, 46.1, 42.0, 20.4 ($-\text{CH}_3$), 14.56 ($-\text{CH}_3$), 14.43 ($-\text{CH}_3$); HRMS (ESI) (m/z) Calcd for $\text{C}_{23}\text{H}_{28}\text{N}_2\text{O}_5$ 413.20710 found 413.20919 (M + H)⁺

Ethyl-2,5-dimethyl-5-(4-(3-phenylbut-2-enoyl)piperazine-1-carbonyl)-4,5-dihydrofuran-3-carboxylate (3l)

It was obtained as a yellow oil; yield: 40% (170.8 mg); IR (ATR) ν_{\max} 3054, 2961, 2916, 2868, 1732 (C=O), 1696

(C=O), 1617 (C=C), 1228, 1097, 750, 706 (arom. CH) cm^{-1} ; ^1H NMR (400 MHz, CDCl_3) δ (ppm): 7.45 (2H, dd, $J = 8.4$, 1.6 Hz, arom. CH), 7.36 (3H, m), 6.26 (1H, s, H_{olef}), 4.16 (2H, q, $J = 7.2$ Hz, $-\text{OCH}_2\text{CH}_3$), 3.91–3.50 (8H, broad), 3.61 (1H, d, $J = 15.2$ Hz, Ha-4), 2.73 (1H, d, $J = 15.2$ Hz, Hb-4), 2.29 (3H, s, $-\text{CH}_3$), 2.19 (3H, s, $-\text{CH}_3$), 1.58 (3H, s, $-\text{CH}_3$), 1.27 (3H, t, $J = 7.2$ Hz, $-\text{OCH}_2\text{CH}_3$); ^{13}C -NMR (100 MHz, CDCl_3) δ (ppm): 171.5 (C=C, C-2), 170.6 (C=O), 165.6 (C=O), 164.5 (C=O), 141.4 (C=C), 128.5, 128.5, 125.9, 118.8 (C=C), 102.3 (C=C, C-3), 88.3, 59.7, 46.3, 43.4, 41.2, 26.0 ($-\text{CH}_3$), 18.03 ($-\text{CH}_3$), 14.37 ($-\text{CH}_3$), 14.07 ($-\text{CH}_3$); HRMS (ESI) (m/z) Calcd for $\text{C}_{24}\text{H}_{30}\text{N}_2\text{O}_5$ 427.22275 found 427.22406 (M + H) $^+$

Ethyl 5-(4-(3,3-diphenylacryloyl)piperazine-1-carbonyl)-2,5-dimethyl-4,5-dihydrofuran-3-carboxylate (3 m)

It was obtained as a yellow oil; yield: 50% (244 mg); IR (ATR) ν_{max} 3054, 2961, 2921, 2863, 1730 (C=O), 1650 (C=O), 1620 (C=C), 1228, 1060, 760, 703 (arom. CH) cm^{-1} ; ^1H NMR (400 MHz, CDCl_3) δ (ppm): 7.37–7.27 (10H, m, arom. CH), 6.30 (1H, s, H_{olef}), 4.15 (2H, q, $J = 6.8$ Hz, $-\text{OCH}_2\text{CH}_3$), 3.52 (1H, d, $J = 15.2$ Hz, H-4), 3.75–2.76 (8H, broad), 2.66 (1H, d, $J = 15.2$ Hz, H-4), 2.15 (3H, s, $-\text{CH}_3$), 1.50 (3H, s, $-\text{CH}_3$), 1.25 (3H, t, $J = 6.8$ Hz, $-\text{OCH}_2\text{CH}_3$); ^{13}C -NMR (100 MHz, CDCl_3) δ (ppm): 172.8 (C=C, C-2), 170.3 (C=O), 167.2 (C=O), 165.6 (C=O), 140.5, 129.5, 128.8, 128.7, 128.4, 128.4, 128.1, 120.0, 110.0 (C=C), 102.3 (C=C, C-3), 88.2, 59.7, 46.1, 45.6, 41.1, 25.9 ($-\text{CH}_3$), 14.3 ($-\text{CH}_3$), 14.0 ($-\text{CH}_3$); HRMS (ESI) (m/z) Calcd for $\text{C}_{29}\text{H}_{32}\text{N}_2\text{O}_5$ 489.23840 found 489.23854 (M + H) $^+$

Ethyl-2,5-dimethyl-5-(4-(3-(thiophen-2-yl)acryloyl)piperazine-1-carbonyl)-4,5-dihydrofuran-3-carboxylate (3n)

It was obtained as a yellow oil; yield: 20% (84 mg); IR (ATR) ν_{max} 3080, 2961, 2916, 2850, 2954, 1734 (C=O), 1694 (C=O), 1631 (C=C), 1236, 1090, 760, 701 (arom. CH) cm^{-1} ; ^1H NMR (400 MHz, CDCl_3) δ (ppm): 7.84 (1H, d, $J = 15.2$ Hz, H_{olef}), 7.34 (1H, d, $J = 4.8$ Hz, arom. CH), 7.23 (1H, d, $J = 4.0$ Hz, arom. CH), 7.05 (1H, d, $J = 4.8$ Hz, arom. CH) 6.65 (1H, d, $J = 15.2$ Hz, H_{olef}), 4.17 (2H, q, $J = 7.2$ Hz, $-\text{OCH}_2\text{CH}_3$), 3.92–3.38 (8H, broad) 3.62 (1H, d, $J = 15.2$ Hz, Ha-4), 2.73 (1H, d, $J = 15.2$ Hz, Hb-4), 2.20 (3H, s, $-\text{CH}_3$), 1.59 (3H, s, $-\text{CH}_3$), 1.28 (3H, t, $J = 7.2$ Hz, $-\text{OCH}_2\text{CH}_3$); ^{13}C -NMR (100 MHz, CDCl_3) δ (ppm): 171.4 (C=C, C-2), 170.3 (C=O), 167.3 (C=O), 165.6 (C=O), 136.4, 130.6, 128.0, 127.5, 114.9 (C=C), 110.0 (C=C, C-3), 88.3, 59.7, 45.4, 42.3, 41.2, 29.68 ($-\text{CH}_3$), 14.37 ($-\text{CH}_3$), 14.09 ($-\text{CH}_3$); HRMS (ESI) (m/z) Calcd for $\text{C}_{21}\text{H}_{26}\text{N}_2\text{O}_5\text{S}$ 419.16352 found 419.16496 (M + H) $^+$

Trans-Ethyl 4-(4-methacryloylpiperazine-1-carbonyl)-2-methyl-5-(thiophen-2-yl)-4,5-dihydrofuran-3-carboxylate (3o)

It was obtained as a yellow oil; yield: 30% (125 mg); IR (ATR) ν_{max} 3085, 2974, 2921, 2863, 1732 (C=O), 1692 (C=O), 1621 (C=C), 1194, 1080, 756, 703 (arom. CH) cm^{-1} ; ^1H NMR (400 MHz, CDCl_3) δ (ppm): 7.33 (1H, dd, $J = 4.8$, 1.2 Hz, arom. CH), 7.17 (1H, dd, $J = 4.8$, 1.2 Hz, arom. CH), 7.00 (1H, dd, $J = 4.8$, 1.2 Hz, arom. CH), 5.90 (1H, d, $J = 7.2$ Hz, H-5), 5.22 (1H, s, H_{olef}), 5.03 (1H, s, H_{olef}), 4.50 (1H, d, $J = 7.2$ Hz, H-4), 4.14 (2H, q, $J = 7.2$ Hz, $-\text{OCH}_2\text{CH}_3$), 3.73–3.50 (8H, broad), 2.29 (3H, s, $-\text{CH}_3$), 1.94 (3H, s, $-\text{CH}_3$), 1.28 (3H, t, $J = 7.2$ Hz, $-\text{OCH}_2\text{CH}_3$); ^{13}C -NMR (100 MHz, CDCl_3) δ (ppm): 171.3 (C=C, C-2), 171.1 (C=O), 168.8 (C=O), 164.8 (C=O), 142.2, 139.9 (C=C), 127.1, 126.3, 126.05, 116.0 (C=C), 103.7 (C=C, C-3), 83.0, 60.0, 53.1, 46.4, 42.7, 20.4 ($-\text{CH}_3$), 14.5 ($-\text{CH}_3$), 14.4 ($-\text{CH}_3$); HRMS (ESI) (m/z) Calcd for $\text{C}_{21}\text{H}_{26}\text{N}_2\text{O}_5\text{S}$ 419.16352 found 419.16443 (M + H) $^+$

Ethyl-2,5-dimethyl-5-(4-(3-(thiophen-2-yl)but-2-enoyl)piperazine-1-carbonyl)-4,5-dihydrofuran-3-carboxylate (3p)

It was obtained as a yellow oil; yield: 20% (86 mg); IR (ATR) ν_{max} 3085, 2987, 2930, 2863, 1734 (C=O), 1694 (C=O), 1620 (C=C), 1194, 1062, 761, 706 (arom. CH) cm^{-1} ; ^1H NMR (400 MHz, CDCl_3) δ (ppm): 7.20 (1H, dd, $J = 3.6$, 0.8 Hz, arom. CH), 7.03–7.01 (2H, dd, $J = 4.8$, 3.6 Hz arom. CH), 6.37 (1H, s, H_{olef}), 4.16 (2H, q, $J = 7.2$ Hz, $-\text{OCH}_2\text{CH}_3$), 3.89–3.50 (8H, broad), 3.59 (1H, d, $J = 15.2$ Hz, Ha-4), 2.72 (1H, d, $J = 15.2$ Hz, Hb-4), 2.33 (3H, s, $-\text{CH}_3$), 2.26 (3H, s, $-\text{CH}_3$), 1.58 (3H, s, $-\text{CH}_3$), 1.27 (3H, t, $J = 7.2$ Hz, $-\text{OCH}_2\text{CH}_3$); ^{13}C -NMR (100 MHz, CDCl_3) δ (ppm): 170.5 (C=C, C-2), 166.6 (C=O), 165.6 (C=O), 164.5 (C=O), 145.1 (C=C), 140.6, 127.8, 126.9, 125.8, 116.25 (C=C), 102.3 (C=C, C-3), 88.3, 59.7, 46.3, 43.5, 41.2, 26.04 ($-\text{CH}_3$), 17.83 ($-\text{CH}_3$), 14.36 ($-\text{CH}_3$), 14.07 ($-\text{CH}_3$); HRMS (ESI) (m/z) Calcd for $\text{C}_{22}\text{H}_{28}\text{N}_2\text{O}_5\text{S}$ 433.17917 found 433.18051 (M + H) $^+$

Method of in vitro AChE inhibition experiments

Slightly modified Ellman method was carried out to determine in vitro AChE inhibitory activities of test compounds [49].

The assay solution was prepared by adding 1480 μL of phosphate buffer (pH = 8.0, 0.1 M), 50 μL of DTNB solution (prepared with pH 7 phosphate buffer), 20 μL of test compounds at desired concentration in ethanol-deionized water (1:1), 10 μL of substrate solution (ATCI, in deionized water) and 25 μL of AChE solution (prepared with

deionized water and 1% gelatin). After that assay solution was incubated for 10 min. at 30 °C and absorbance at 412 nm was determined.

A control solution containing all compounds except inhibitor was performed same as above and the absorbance at 412 nm was considered 100% enzyme activity.

The percentage activity of AChE for any tested compound at desired concentration was calculated with the formula:

$$\% \text{ enzyme activity} = (A_s/A_0) \times 100$$

A_s : Absorbance of assay solution with inhibitor.

A_0 : Absorbance of control solution.

The concentration of each test compound was tested in triplicate and IC_{50} values were calculated graphically using GraphPad Prism 8.0.3 software. IC_{50} value is defined as the concentration of sample which performs 50% inhibition towards AChE.

Methods of in silico molecular docking experiments

Three dimensional structure of recombinant human AChE complexed with Donepezil was obtained from the Protein Data Bank (4EY7) [50]. B-chain, water molecules, and detergents were removed. Conformational analysis of inhibitor test compounds were performed with Avogadro software and most stable conformations were optimized with semiempirical PM6 method in Gaussian 09 Software. All ligand-protein docking calculations were performed as a flexible ligand in rigid protein using AutoDock Vina software [51]. Best docking mod of ligand in terms of binding energy (Kcal/mol) was selected and used.

According to these results, it can be seen that all piperazine-dihydrofuran AChEI compounds present satisfactory druglike properties, including our lead compound **3j**.

Acknowledgements This study was financially supported by the Scientific and Technical Research Council of Turkey (TUBITAK) (TBAG-116Z455). Sait SARI thanks to TUBITAK for doctoral fellowship.

Compliance with ethical standards

Conflict of interest The authors declare no competing interests.

Publisher's note Springer Nature remains neutral with regard to jurisdictional claims in published maps and institutional affiliations.

References

- Alzheimer's Association. Alzheimer's disease facts and figures. *Alzheimers Dement.* 2017;2017:325–73.
- He Q, Liu J, Lan J, Ding J, Sun Y, Fang Y, Jiang N, Yang Z, Sun L, Jin Y, Xie S. Coumarin-dithiocarbamate hybrids as novel multitarget AChE and MAO-B inhibitors against Alzheimer's disease: design, synthesis and biological evaluation. *Bioorg Chem.* 2018;81:512–28.
- Wortmann M. World Alzheimer report 2014: dementia and risk reduction. *Alzheimers Dement.* 2014;11:837.
- Hampel H, Mesulam MM, Cuello A, Khachaturian AS, Vergallo A, Farlow MR, Snyder PJ, Giacobini E, Khachaturian ZS. Revisiting the cholinergic hypothesis in Alzheimer's disease: emerging evidence from translational and clinical research. *J Prev Alzheimers Dis.* 2019;6:2–15.
- Mufson EJ, Ikonovic MD, Counts SE, Perez SE, Ahmadi MM, Scheff WS, Ginsberg SD. Molecular and cellular pathophysiology of preclinical Alzheimer's disease. *Behav Brain Res.* 2016;311:54–69.
- LaFerla F, Green K, Oddo S. Intracellular amyloid- β in Alzheimer's disease. *Nat Rev Neurosci.* 2007;8:499–509.
- Dumas JA, Newhouse PA. The cholinergic hypothesis of cognitive aging revisited again: cholinergic functional compensation. *Pharm Biochem Behav.* 2011;99:254–61.
- Akasofu S, Kimura M, Kosasa T, Sawada K, Ogura H. Study of neuroprotection of donepezil, a therapy for Alzheimer's disease. *Chem Biol Interact.* 2008;175:222–6.
- Molinuevo JL, Gauthier S. Benefits of combined cholinesterase inhibitor and memantine treatment in moderate-severe Alzheimer's disease. *Alzheimers Dement.* 2013;9:326–31.
- Tougu V. Acetylcholinesterase: mechanism of catalysis and inhibition. *Curr Med Chem.* 2001;1:155–70.
- Rashid U, Ansari FL. Challenges in designing therapeutic agents treating Alzheimer's disease-form serendipity to rationality. *Drug Design Discovery in Alzheimer's Disease.* Elsevier; 2015.
- Sugimoto H, Iimura Y, Yamanishi Y, Yamatsu K. Synthesis and structure-activity relationships of acetylcholinesterase inhibitors: 1-benzyl-4-[(5,6-dimethoxy-1-oxindan-2-yl)methyl]piperidine hydrochloride and related compounds. *J Med Chem.* 1995;38:4821–9.
- Weintraub D, Somogyi M, Meng X. Rivastigmine in Alzheimer's disease and Parkinson's disease dementia: an ADAS-cog factor analysis. *Am J Alzheimers Dis Other Dement.* 2011;26:443–9.
- Giacobini E. Cholinesterase inhibitors: new roles and therapeutic alternatives. *Pharm Res.* 2004;50:433–40.
- Taylor AP, Robinson RP, Fobian YM, Blakemore DC, Jones LH, Fadeyi O. Modern advances in heterocyclic chemistry in drug discovery. *Org Biomol Chem* 2016;14:6611–37.
- Szabo M, Herenbrink CK, Christopoulos A, Lane JR, Capuano B. Structure-activity relationships of privileged structures lead to the discovery of novel biased ligands at the dopamine D2 receptor. *J Med Chem.* 2014;57:4924–39.
- Meena P, Nemaish V, Khatri M, Manral A, Luthra PM, Tiwari M. Synthesis, biological evaluation and molecular docking study of novel piperidine and piperazine derivatives as multi-targeted agents to treat Alzheimer's disease. *Bioorg Med Chem* 2015;23:1135–48.
- Piemontese L, Tomás D, Hiremathad A, Capriati VI, Candeias E, Cardoso SM, Chaves S, Santos MA. Donepezil structurebased hybrids as potential multifunctional anti-Alzheimer's drug candidates. *J Enzym Inhib Med Chem.* 2018;33:1212–24.
- Demirayak Ş, Şahin Z, Ertaş M, Bülbül EF, Bender C, Biletekin SN, Berk B, Sağlık BN, Levent S, Yurttaş L. Novel thiazole-piperazine derivatives as potential cholinesterase inhibitors. *J Heterocycl Chem.* 2019;56:3370–86.
- Chen SP, Chen BW, Dai CF, Sung PJ, Wu YC, Sheu JH, Sarcophytonins F, New G. Dihydrofuranocembranoids from a Dongsha Atoll Soft Coral Sarcophyton sp. *Bull Chem Soc Jpn.* 2012;85:920–2.
- Lallemand JY, Six Y, Ricard LA. Concise synthesis of an advanced clerodin intermediate through a vauquier tandem reaction. *Eur J Org Chem.* 2002;3:503–13.

22. Melikyan GG. Manganese(III) mediated reactions of unsaturated systems. *Synthesis*. 1993;9:833–50.
23. Mondal M, Bora U. Recent advances in manganese(III) acetate mediated organic synthesis. *RSC Adv*. 2013;3:18716–54.
24. Castro S, Fernandez JJ, Fananas FJ, Vicente R, Rodriguez F, Manganese-Mediated C-H. Alkylation of unbiased arenes using alkylboronic acids. *Chem Eur J* 2016;22:9068–71.
25. Lofstrand VA, Matsuura BS, Furst L, Narayanam JMR, Stephenson JRC. Formation and trapping of azafulvene intermediates derived from manganese-mediated oxidative malonate coupling. *Tetrahedron* 2016;72:3775–80.
26. Aslan H, Öktemer A, Dal H, Hökelek T. Synthesis of ferrocene substituted dihydrofuran derivatives via manganese(III) acetate mediated radical addition-cyclization reactions. *Tetrahedron* 2017;73:7223–32.
27. Hyunh TT, Nguyen VH, Nishino H. One-pot synthesis of 2-oxa-7-azaspiro[4.4]nonane-8,9-diones using Mn(III)-based oxidation of 4-acylpyrrolidine-2,3-diones. *Tetrahedron Lett*. 2017;58:3619–22.
28. Zhang PZ, Zhang L, Li JA, Shoberu A, Zou JP, Zhang W. Phosphinoyl radical initiated vicinal cyanophosphinoylation of alkenes. *Org Lett*. 2017;19:5537–40.
29. Kobayashi K, Nagase K, Morikawa O, Konishi H. Convenient synthesis of furopyranopyrandione derivatives by the can-mediated furan ring formation. *Heterocycles* 2003;60:939–46.
30. Chuang CP, Wu YL. Oxidative free radical reactions of enamino esters. *Tetrahedron* 2004;60:1841–7.
31. Nair V, Mohanan K, Suja TD, Suresh E. Stereoselective synthesis of 3,4-trans-disubstituted pyrrolidines and cyclopentanes via intramolecular radical cyclizations mediated by CAN. *Tetrahedron Lett*. 2006;47:2803–6.
32. Hocaoglu B, Yilmaz M. Regioselective radical addition of 3-oxopropanenitriles with terminal dienes promoted by cerium(IV) ammonium nitrate and manganese(III) acetate. *Synth Commun*. 2019;49:1938–46.
33. Ustalar A, Yilmaz M. Microwave assisted synthesis of 2,3-dihydro-4*H*-benzo[4,5]thiazolo[3,2-*a*]furo[2,3-*d*]pyrimidin-4-ones and 6,7-dihydro-5*H*-furo[2,3-*d*]thiazolo[3,2-*a*]pyrimidin-5-ones using Mn(OAc)₃. *Tetrahedron Lett* 2017;58:516–9.
34. Yilmaz M, Bicer E, Ustalar A, Pekel AT. Synthesis of furan-substituted dihydrofuran compounds by radicalcyclization reactions mediated by manganese(III) acetate. *Arkivoc* 2014;v:225–36.
35. Özgür M, Yilmaz M, Nishino H, Avar EÇ, Dal H, Pekel AT, Hökelek T. Efficient syntheses and antimicrobial activities of new thiophene containing pyranone and quinolinone derivatives using manganese(III) acetate: the effect of thiophene on ring closure–opening reactions. *N. J Chem*. 2019;43:5737–51.
36. Yilmaz EVB, Yilmaz M, Öktemer A. Radical cyclizations of conjugated esters and amides with 3-oxopropanenitriles mediated by manganese(III) acetate. *Arkivoc* 2011;ii:363–76.
37. Yilmaz M, Ustalar A, Uçan B, Pekel AT. Regio- and diastereoselective synthesis of trans-dihydrofuran-3-carboxamides by radical addition of 1,3-dicarbonyl compounds to acrylamides using manganese(III) acetate and determination of exact configuration by X-ray crystallography. *Arkivoc* 2016;vi:79–91.
38. Sari S, Yilmaz M. Synthesis, characterization, acetylcholinesterase inhibition, and molecular docking studies of new piperazine substituted dihydrofuran compounds. *Med Chem Res* 2020;29:1804–18.
39. Snider BB. Manganese(III)-based oxidative free-radical cyclizations. *Chem Rev*. 1996;96:339–63.
40. Pan W, Hu K, Bai P, Yu L, Ma Q, Li T, Zhang X, Chen C, Peng K, Liu W, Sang Z. Design, synthesis and evaluation of novel ferulic acid-memoquin hybrids as potential multifunctional agents for the treatment of Alzheimer's disease. *Bioorg Med Chem Lett*. 2016;26:2539–43.
41. Shaik JB, Yeggoni DP, Kandrakonda YR, Penumala M, Zinka RB, Kotapati KV, Darla MM, Ampasala DR, Subramanyam R, Amooru DG. Synthesis and biological evaluation of flavone-8-acrylamide derivatives as potential multi-target-directed anti Alzheimer agents and investigation of binding mechanism with acetylcholinesterase. *Bioorg Chem*. 2019;88:102960.
42. Estrada M, Herrera-Arozamena C, Perez C, Vina D, Romero A, Morales-Garcia JA, Castillo AP, Rodriguez-Franco MI. New cinnamic – N-benzylpiperidine and cinnamic – N,N-dibenzyl(N-methyl)amine hybrids as Alzheimer-directed multitarget drugs with antioxidant, cholinergic, neuroprotective and neurogenic properties. *Eur J Med Chem*. 2016;121:376–86.
43. Singh YP, Tej GNVC, Pandey A, Priya K, Pandey P, Shankar G, Nayak PK, Rai G, Chittiboyina AG, Doerksen RJ, Vishwakarma S, Modi G. Design, synthesis and biological evaluation of novel naturally-inspired multifunctional molecules for the management of Alzheimer's disease. *Eur J Med Chem*. 2020;198:112257.
44. Fu J, Bao F, Gu M, Liu J, Zhang Z, Ding J, Xie S, Ding J. Design, synthesis and evaluation of quinolinone derivatives containing dithiocarbamate moiety as multifunctional AChE inhibitors for the treatment of Alzheimer's disease. *J Enzym Inhib*. 2020;35:118–28.
45. Wiesner J, Kriz Z, Kuca K, Jun D, Koca J. Acetylcholinesterases – the structural similarities and differences. *J Enzym Inhib Med Chem*. 2007;22:417–24.
46. Lipinski CA, Lombardo F, Dominy BW, Feeney PJ. Experimental and computational approaches to estimate solubility and permeability in drug discovery and development settings. *Adv Drug Deliv Rev*. 1997;23:3–25.
47. Lipinski CA, Lombardo F, Dominy BW, Feeney PJ. Experimental and computational approaches to estimate solubility in drug discovery and development settings. *Adv Drug Deliv Rev*. 2001;46:3–26.
48. Sari S, Ünal S, Yilmaz M. Synthesis and characterization of unsaturated diacyl and alkyl-acyl piperazine derivatives. *Turk J Chem*. 2019;43:1656–71.
49. Ellman GL, Courtney KD, Andres V Jr, Featherstone RM. A new and rapid colorimetric determination of acetylcholinesterase activity. *Biochem Pharm*. 1961;7:90–95.
50. Cheung J, Rudolph MJ, Burshteyn F, Cassidy MS, Gary EN, Love J, Franklin MC, Height JJ. Structures of human acetylcholinesterase in complex with pharmacologically important ligands. *J Med Chem*. 2012;55:10282–6.
51. Trott O, Olson AJ. AutoDock Vina: improving the speed and accuracy of docking with a new scoring function, efficient optimization and multithreading. *J Comput Chem*. 2010;31:455–461.